Structure of iodine–nylon 6 complex: 2. Arrangement of polyiodides in the complex

Akio Kawaguchi
Research Reactor Institute, Kyoto University, Kumatori-cho, Sennan-gun, Osaka 590-04, Japan
(Received 27 September 1993; revised 2 November 1993)

Doubly oriented iodine-doped nylon 6 (iodine–nylon 6 complex) was prepared by immersing nylon 6 in an I_2–KI aqueous solution and was studied using X-ray diffraction. The intensities in the X-ray diffraction pattern from the iodine-doped nylon 6 vary with ageing time after doping. The variation is attributed to the rearrangements of polyiodides in the complex. In the complex two kinds of 'one-dimensional' ordered structures give streaks on the layer lines, and a three-dimensional ordered structure (complex crystal) gives Bragg reflections. Just after doping an unstable 'one-dimensional' structure emerges. This subsequently transforms into a stable 'one-dimensional' structure and/or the three-dimensional complex crystal with ageing. The arrangement of polyiodides in the complex has been determined. The unstable 'one-dimensional' structure is incommensurate with the complex crystal; a structural model based on co-ordination of I_2 with I_3^- is proposed on the basis of the intensities of the unstable streaks vanishing with ageing. The complex crystal is concluded to include I_3^- ions inclining at an angle to the chain axis of nylon 6. The stable 'one-dimensional' structure contains I_5^- ions which are oriented parallel to the chain axis.

(Keywords: iodine; nylon 6; complex crystal)

INTRODUCTION

Iodine-doped nylon 6 (iodine–nylon 6 complex) is an intermediate state formed as the α-form of nylon 6 transforms to the γ-form. The transition is induced by iodine doping in an iodine–potassium iodide (I_2–KI) aqueous solution and desorption of iodine in a sodium thiosulfate aqueous solution[1–6].

Hydrogen bonds are formed between antiparallel chains in the α-form of nylon 6 and are formed between parallel chains in the γ-form[2]. Hence it has been argued that iodine doping induces the conversion of hydrogen bonds in the α-form into those of the γ-form. It is believed that iodine atoms or polyiodide ions, I_n^-, are arranged between the hydrogen-bonded planes of the α-form and weaken the hydrogen bonds between antiparallel chains. In fact, hydrostatic compression of the complex crystal shows that the compressibility has lost anisotropy around the chain axis[7,8]. Murthy *et al.* reported the structure of the complex studied with X-ray diffraction, Raman spectroscopy and n.m.r.[9–12]. They proposed several models for the structure of the complex; for example, I_3^- and I_5^- ions lie between the hydrogen-bonded planes and are co-ordinated to weaken the hydrogen bonds. However, the structure of the complex has yet to be fully determined.

In a previous paper, we investigated doubly oriented iodine–nylon 6 complexes with X-ray diffraction and determined the unit cell of the complex crystal[7]: a monoclinic unit cell with the space group $P2_1/a$ or $P2_1$, $a=0.913$ nm. $b=1.62$ nm (chain axis), $c=1.79$ nm and $\beta=59.7°$. The length of the b-axis (chain axis) is almost the same as that of the γ-form (1.67 nm) and much shorter than that of the α-form (1.72 nm)[1,2]. The complex shows not only crystalline reflections but also strong diffuse scatterings on the layer lines[9–12]. The X-ray diffraction intensities of both the crystalline reflections and the diffuse scatterings change remarkably with ageing after iodine doping; polyiodides in doped nylon 6 change their arrangement. In this paper, the structure of the complex will be investigated on the basis of X-ray diffraction; in particular, the arrangement of polyiodides in doped nylon 6 is studied taking into account the X-ray diffraction along the meridian.

EXPERIMENTAL

A film of doubly oriented nylon 6 was immersed in a 0.1 N I_2–KI aqueous solution to obtain a film of doubly oriented complex. The details of the process have been reported previously[7].

The amount of absorbed iodide depends on the film; the highest increase in weight with doping amounts to 230%. The time required to achieve the doping differs from sample to sample; some samples can be doped in several minutes and others cannot be doped in several months. Doping was uniform along the film thickness as confirmed by optical microscopy of a cross-section of the specimen.

Ageing after iodine doping was carried out in an air atmosphere at room temperature. Some samples were aged in saturated I_2 vapour at atmospheric pressure to prevent volatilization of I_2.

For Raman spectroscopy, the doubly oriented specimen was set in a cryostat at liquid nitrogen temperature. The incident beam was the 514.5 nm line from an argon laser

0032-3861/94/12/2665–07

(200 mW). The incident beam was normal to the surface of the specimen and the Raman spectra were obtained from the 180° scattered light through a double monochromator (Spex model 1402). The incident beam and scattered light were polarized parallel or perpendicular to the chain axis of the specimen.

X-ray diffraction photographs were taken with a flat-film camera with Mo Kα radiation (0.0711 nm) monochromatized by a graphite monochromator. For intensity measurements along the meridian with a diffractometer, Cu Kα radiation (0.154 nm) filtered with a nickel foil (0.1 mm thick) was used. The step-scanning method was adopted in (θ–2θ) scanning from 5 to 50° of 2θ with 0.12 or 0.09° per step. The instrumental breadth of the incident X-ray was estimated to be 0.2° in 2θ. Doubly oriented doped samples were ~0.2 mm thick; the attenuations of intensity for Mo Kα through the sample film were 40 and 30% for a fresh sample and that aged for several months, respectively.

Background intensities including amorphous scattering and Compton scattering are assumed to be a smooth curve passing through minimum points of the Bragg reflections and the streaks, and are subtracted from the measured intensities to give the observed intensity, I_{obs}. The observed intensity, I_{obs}, was corrected to give an intensity, I_0, which is a square of the geometric structure factor, F_0.

$$I_{obs} = k_0 I_0 A(\theta) B(\theta) P(\theta) \quad (1)$$

where $A(\theta)$, $B(\theta)$ and k_0 are an absorption factor, the atomic scattering factor of iodine and a scale factor, respectively; $P(\theta)$ is the polarization factor and the Lorentz factor for oriented sample $[=(1+\cos^2 2\theta)/2\sin 2\theta]$. Since the scattering amplitude of an iodine atom is much greater than that of the elements included in nylon 6, only iodine is taken into consideration for the calculation of the intensity; the iodine atom has a scattering power more than 40 times that of carbon, oxygen, nitrogen or hydrogen atoms.

RESULTS

Figure 1 shows the Raman spectra of the iodine–nylon 6 complex with the light polarized parallel and perpendicular to the chain axis (*b*-axis). The spectra agreed well with those reported by Murthy *et al.*; the band assigned to I_5^- (170 cm^{-1}) was observed only with the incident beam polarized parallel to the chain axis while the band at 115 cm^{-1} (assigned to I_3^-) was observed with both parallel and perpendicular polarization. Hence, linear I_5^- ions exist in the complex with their long axes parallel to the chain axis, while the components of the long axes of I_3^- ions are both parallel and perpendicular to the chain axis and/or may exist in the amorphous fraction. There was no appreciable change in the ratio of the two bands 6 months after iodine doping, while the absolute intensities decreased, thus suggesting no change in the iodine species in the observed region for Raman spectroscopy with ageing.

In X-ray scattering of the doubly oriented iodine–nylon 6 complex, two kinds of scattering were observed: Bragg reflections and diffuse scattering. With the incident X-ray perpendicular to the chain axis (*b*-axis), 0*kl* Bragg reflections and several streaks are observed on layer lines (*Figure 2*). The intensities of these streaks and of the Bragg reflections change with ageing after iodine doping without any shift in the peak positions (*Figure 2b*). These changes in intensity are also observed in ageing in saturated I_2 vapour and air, and hence the change in the structure cannot be attributed to the volatilization of I_2. The 02*l* and 04*l* Bragg reflections are weak just after iodine doping and become stronger and clearer with ageing for one or several days in the atmosphere. On the other hand, the equatorial 00*l* reflections are much clearer than the off-equatorial 02*l* or 04*l* reflections just after the doping and decrease in intensity for odd *l* with ageing. Since the 02*l* or 04*l* reflections do not show any appreciable change in intensity with *l*, the 00*l* reflections are attributed not only to the complex crystal but also to other structures in the complex.

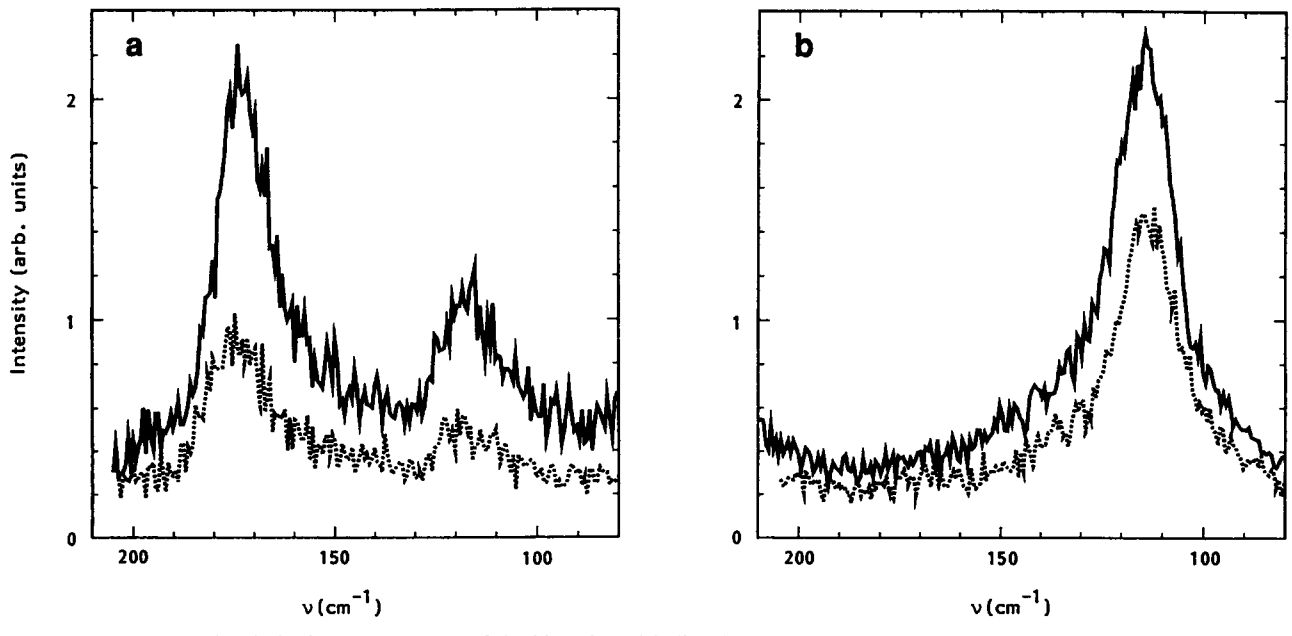

Figure 1 Back-scattered polarized Raman spectra of doubly oriented iodine-doped nylon 6 with incident beam perpendicular to film surface. Incident beam and scattered light polarized (a) parallel and (b) perpendicular to the chain axis (—, just after iodine doping; ···, 6 months after doping)

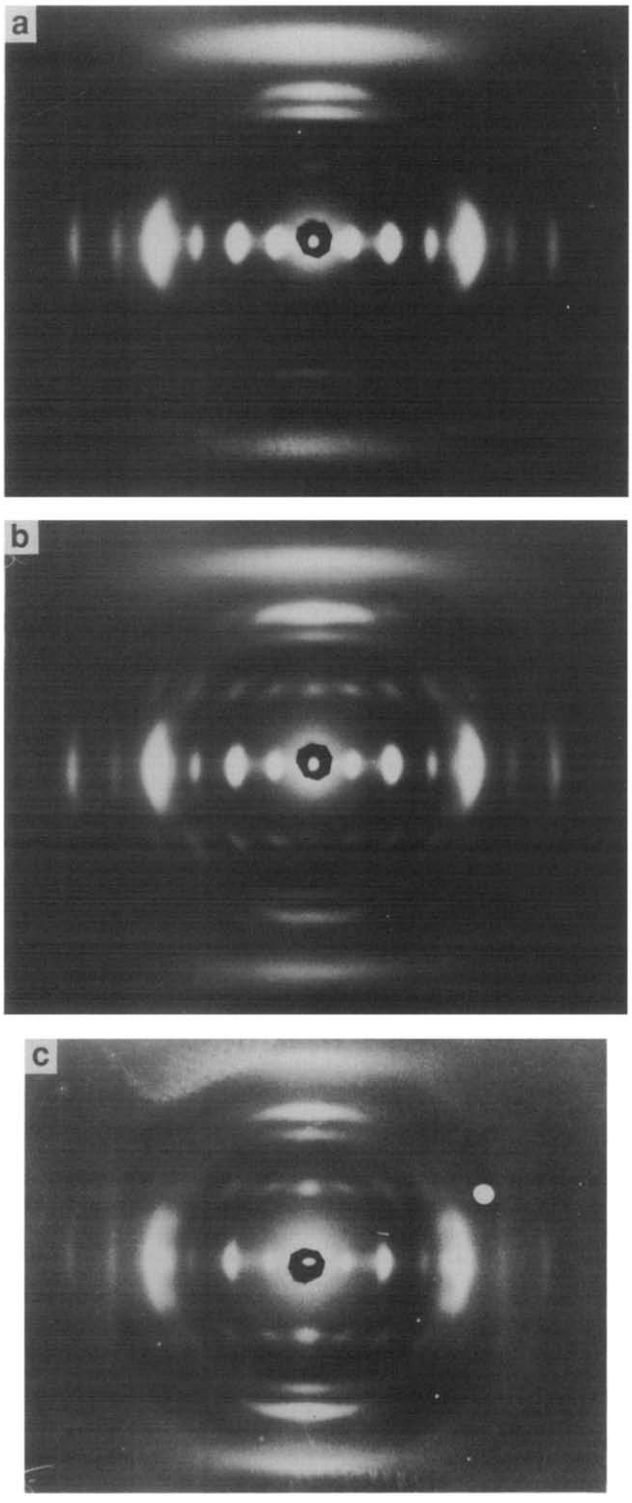

Figure 2 X-ray photographs of doubly oriented complex films: (a) just after iodine doping; (b and c) 1 day after doping. Incident X-ray (a and b) parallel and (c) perpendicular to film surface. The meridian is the chain axis

Figures 2a and *b* show the change in the diffuse scatterings with ageing. The layer line streaks at $q = 2.12$, 3.13 and 5.35 nm^{-1} ($q = 2 \sin\theta/\lambda$) away from the equator decrease in intensity with ageing; they are unstable streaks. An iodine-doped sample aged for 8 months in the atmosphere recovers the unstable streaks after being treated again in the I_2–KI solution for 30 min; the structure giving the unstable streaks is formed and stabilized only in the I_2–KI solution. On the other hand, the intensity of a streak at 3.3 nm^{-1} remains unchanged or increases: it is a stable streak. Furthermore, in *Figure 2c* there are two row-line streaks perpendicular to the equator at 3.2 and 4.4 nm^{-1} away from the meridian with the incident X-ray normal to the film surface. A change in the intensities of these row-line streaks, however, is not clarified because they are occasionally superimposed on the Bragg reflections.

Table 1 shows the peak position (2θ) for the Bragg reflections and layer-line streaks on the meridian. *Figures 3a* and *b* show the diffraction profiles along the meridian for the sample just after doping and for that aged for 1 day, respectively. The widths of the layer-line streaks are almost the same as those for the Bragg reflections while the streak at 3.13 nm^{-1} is much broader than that at 2.12 nm^{-1}. Consequently, the streaks are attributed to 'one-dimensional' structure ordered along the chain axis. *Table 1* also lists the corrected intensities of the three Bragg reflections (020, 040 and 080).

DISCUSSION

Bonding in polyiodide

One of the specificities for iodine or any halogen is a co-ordinate bond; iodide ions, iodine molecules or polyiodides (for example, I_2, I_3^- or I_5^-) may form networks through co-ordinate bonds and covalent bonds with other iodine atoms[13,14]. The co-ordination allows the distance between the iodine atoms to be less than twice that of the van der Waals radius of an iodine atom even if the atoms do not form covalent bonds; the distance between iodine atoms in polyiodides is between 0.26 nm (I–I distance for the covalent bond in an I_2 molecule) and 0.34 nm (for the co-ordinate bond in zigzag-chained polyiodide), while the van der Waals radius of an iodine atom is 0.21 nm[13,14]. An ordinary linear I_3^- ion has a cylindrical shape; the length of the long axis is $\sim$1.0 nm. The lengths of a linear I_5^- ion and I_2 are $\sim$1.6 and $\sim$0.7 nm, respectively. The diameter of these cylindrical polyiodides is estimated at $\sim$0.4 nm.

In the following, I_3^- ions with their long axes parallel, perpendicular and inclining at an angle to the chain axis are denoted by I_3^-(para), I_3^-(perp) and I_3^-(incl), respectively.

Diffuse streaks on layer lines

The streaks confined on the layer lines generally suggest two kinds of 'one-dimensional' structure; one is a defect structure coherent with the complex crystal ordered three-dimensionally, such as periodic longitudinal displacements from regular positions; the other is a random linear arrangement of iodine independent of the complex crystal. The former gives streaks commensurate with the Bragg reflection of the crystal. However, the latter may give streaks at incommensurate positions.

The unstable streaks, at 2.12, 3.13 and 5.35 nm^{-1}, are assigned to 2nd, 3rd and 5th order of 1/0.94 nm^{-1}, respectively, while the stable streak is located at 3.3 nm^{-1}. Since the reciprocal of the length of the chain axis (*b*-axis) in the complex crystal is 1/1.62 nm^{-1}, the period for the unstable streaks is incommensurate with the periods both for the stable streak and for the complex crystal.

Therefore, there should be at least three independent structures along the chain axis in the iodine-doped nylon 6: (1) the stable 'one-dimensional' structure which is formed on doping and remains unchanged and/or rather grows with ageing in the atmosphere after doping; (2) the

Table 1 Peak positions and spacings of meridional scatterings in X-ray photographs with corrected intensities of peaks, at 1.26, 2.5 and 5.0 nm^{-1} in *Figure 3b*

	Bragg reflection				Unstable streak				Stable streak
	020	040	060	080					
2θ(deg)[a]	11.2	22.0	(–)[b]	45.2	18.8	28.0	38.7	48.6	30.0
q(nm^{-1})	1.26	2.48	(–)	5.0	2.12	3.13	4.2	5.35	3.3
d(nm)	0.791	0.404	(–)	0.201					
Intensities (arb. units)[c]	1	16.4	0	3.45					

[a] For CuKα radiation
[b] Intensity too weak to be measured
[c] For specimen aged after doping

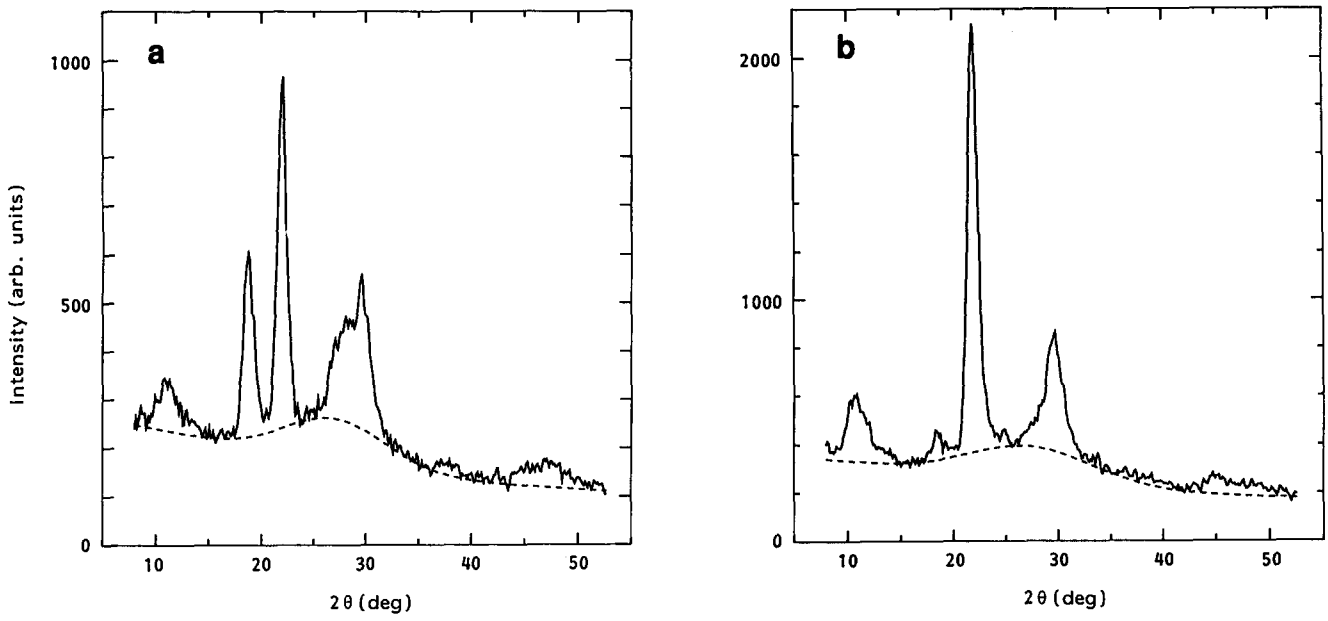

Figure 3 X-ray profile of doubly oriented complex scanned along the meridian (chain axis): (a) just after doping; (b) 1 day after doping (– – –, subtracted background)

unstable 'one-dimensional' structure which is stable only in coexistence with the I_2–KI solution and disappears with ageing in the atmosphere; (3) the three-dimensionally ordered structure giving the Bragg reflections, the complex crystal, which is hardly formed in doping but grows with ageing.

Unstable structure

The unstable streaks can easily be separated from the Bragg reflections and the stable streaks; the corrected intensity profile for the unstable structure is obtained by subtracting the intensity profile around the unstable streaks of the well aged specimen from that of the as-doped one after normalizing the profiles in *Figure 3a* and *b*. *Figure 4* shows a corrected intensity profile of the unstable streaks; strong peaks corresponding to 2nd, 3rd and 5th orders of 1.06 ($=1/0.94$) nm^{-1} and a weak peak of 4th order are observed; the ratios of these intensities do not change appreciably between samples. The peak for the 2nd order is much sharper than that for the 3rd order. Accordingly, the unstable state should consist of a linear arrangement of various structural units with a weight-averaged length of 0.94 nm.

In the period of 0.94 nm, we can accommodate I_3^-(perp), I_3^-(para) or I_2 co-ordinated with I_3^-(perp). The

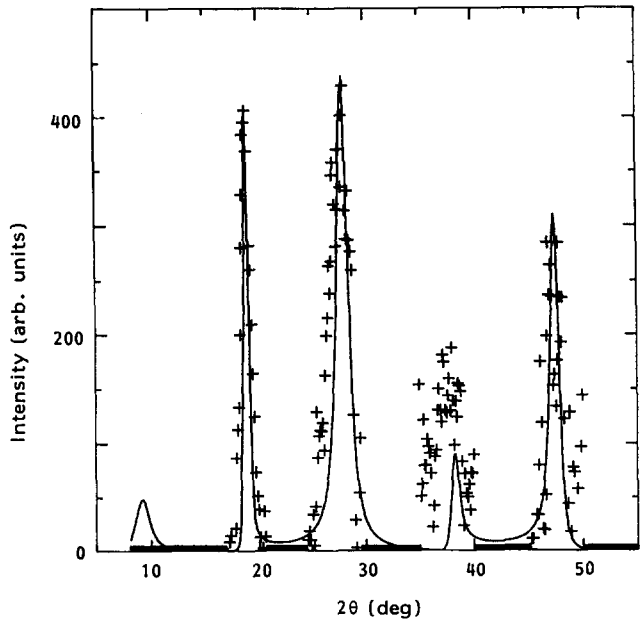

Figure 4 Intensity profile of unstable streaks: (+) corrected experimental profile; (—) profile of I_{calc} which is calculated using the model shown in *Figure 5* ($R_A = 0.425$ nm, $R_B = 0.95$ nm, $r_{B1} = 0.335$ nm, $r_{B2} = 0.28$ nm, ε_A:ε_B = 20:80)

I_5^- ion can be safely discarded because it is too long (>1.6 nm). Thus several models were constructed for the unstable structure using these three species by trial and error.

First, I_3^-(para) ions were arranged along the chain axis. Since its length is ~1.0 nm, other polyiodides cannot be stacked together in a cell. The profile shown in *Figure 4* could not be reproduced even qualitatively by this model though it gives a strong peak for the 3rd order streak. Hence, I_3^-(para) is also discarded in constructing a model for the unstable structure.

Next, several models with I_3^-(perp) and I_2 were considered. A successive stack of I_2 is forbidden because co-ordination between I_2 molecules cannot occur while I_2 can be co-ordinated with I_3^- (ref. 14). Thus, this model is a statistically random stack of two components; $\{I_3^-(\text{perp})\}$ (cell *A* in *Figure 5*) and $\{I_3^-(\text{perp})+I_2\}$ (cell *B*). The latter component with a length of 0.95 nm ($=R_B$) can be regarded as I_3^-(perp) co-ordinated with I_2 parallel to the *b*-axis (or L-shaped bent I_5^-). The latter has a length of 0.425 nm ($=R_A$) (*Figure 5*). This length is close to half that of cell *B*, thus making the peak at 2.12 nm^{-1} sharper than that at 3.13 nm^{-1}.

The calculated intensity profile of this model, I_{calc}, is based on a theory for diffuse scattering by a linear stack of various components with disorder along an axis; the theory is developed by Kakinoki and Komura[15] and extended to linearly disordered crystals by Scaringe and Ibers[16]. The theory requires several parameters including the composition of the components (see Appendix).

The calculated intensity profile was convoluted with a function for instrumental broadening: a Lorentzian with a width of 0.2° in 2θ. *Figure 4* shows both the calculated intensity profile, I_{calc}, and the experimental profile. The calculated profile reproduces the experimental one fairly well; the peak of the 1st order around 10° in 2θ is too weak to be separated experimentally from the strong 020 reflection of the complex crystal, and the peak intensity of the 4th order obtained experimentally suffers larger errors in separating the peak. The best-fitted parameters used are shown in the caption of *Figure 4*. The parameters for the calculation show that the component $\{I_3^-(\text{perp})+I_2\}$ is dominant in the unstable structure; I_2 is stabilized by co-ordination.

Raman spectra of the complex do not show the existence of I_2 molecules. However, Raman scattering occurs at the surface of the complex because of the severe absorption of the incident light. Since the unstable structure in the surface area transforms rapidly to the stable structure or the complex crystal after the doping, the Raman spectra cannot determine the species in the unstable structure, while X-ray scattering can occur all through the specimen; even if I_2 molecules exist in the unstable structure, their stretching mode would not be detected by the present Raman spectroscopy.

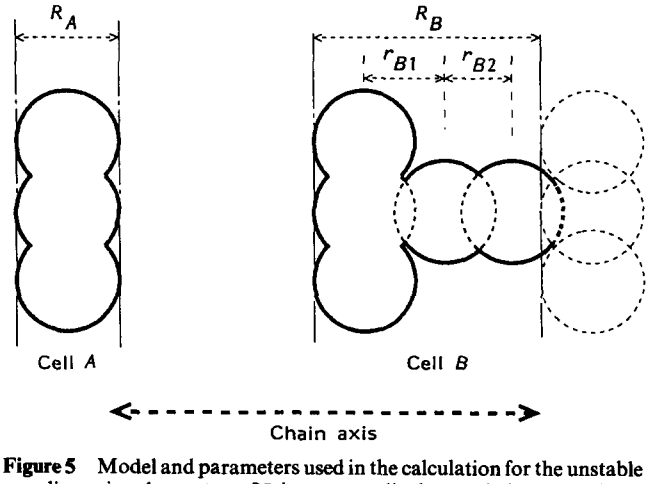

Figure 5 Model and parameters used in the calculation for the unstable one-dimensional structure: I_3^- ion perpendicular to chain axis (cell *A*); I_3^- ion co-ordinated with I_2 (cell *B*)

Complex crystal and stable one-dimensional structure

In the complex crystal the intensity of the 040 reflection is about 16 times stronger than that of the 020 reflection (*Table 1*). The intensity of the 060 reflection is very weak. Hence, the model for the complex crystal should give a strong intensity for the 040 reflection. Though Murthy *et al.*[9–12] assigned the reflection at 2.5 nm^{-1} to the 040 reflection from the α-form of nylon 6, the α-form should give the 020 reflection which is stronger than the 040 reflection, if that were the case. We therefore assign the reflection at 2.5 nm^{-1} to be due to the complex and not to nylon 6.

The Raman spectra suggest the existence of I_3^- and I_5^-. We have discarded I_2 molecules in constructing the model for the complex crystal; if I_2 molecules were to exist, they should be detected by Raman spectroscopy for the stable structures such as the complex crystal and the stable one-dimensional structure. The complex crystal has the space group[7] $P2_1$ or $P2_1/a$. If I_3^- or I_5^- are parallel to the chain axis in the complex crystal with the space group $P2_1$, the following five cases are possible for the unit cell taking into account the volume of the polyiodides: (1) two I_3^-(para); (2) two I_5^-; (3) four I_3^-(para); (4) four I_5^-; (5) two I_3^-(para) and two I_5^-. Cases (3) and (4) can be also applied for the case with the space group $P2_1/a$. However, for these five cases including the polyiodides arranged parallel to the chain axis, the calculation of intensities could not reproduce a strong intensity for the 040 reflection using reasonable values for the intramolecular distances between iodine atoms, though strong 060 or 080 reflections were obtained: for I_3^-(para) ($r_1=0.29$ nm) and I_5^- ($r_{21}=0.33$ nm, $r_{22}=0.27$ nm, see *Figure 6*)[13]. With the calculated results for these five cases, the complex crystal should not contain either I_3^-(para) or I_5^-. On the other hand, I_3^-(perp) ions also cannot be accommodated in the unit cell since the length of an I_3^- ion is ~1.0 nm, longer than the *a*-axis (0.91 nm).

Here, we have introduced I_3^-(incl) the long axis of which makes an angle not equal to 90° with the chain axis. Calculated intensities of 0*k*0 ($k=2,4,6,8$) reflections for I_3^-(incl), which makes an angle of 73° to the axis, are shown in *Figure 6* as a function of a shift distance between two independent I_3^-(incl) ions under the symmetry of $P2_1$: a bond length projected to the axis, 0.085 nm. The shift parameters indicated by the arrows in *Figure 7* can reproduce the intensities of the 0*k*0 Bragg reflections: $I(020):I(040):I(060):I(080)=1:16.7:0.06:3.29$ for the shift of the independent I_3^-(incl) molecules, $d=0.37$ or 0.44 nm. These ratios well reproduce the experimental ones, 1:16.4:0:3.5 (*Table 1*).

The hydrogen bonds in the α-form of nylon 6 are staggered along the *a*-axis in a hydrogen-bonded plane. If an I_3^- ion co-ordinates with the hydrogen bonds, it should be arranged to incline to the chain axis with an angle of ~75° (*Figure 6*): approximately the same angle as that proposed. Furthermore, the hydrogen-bonded

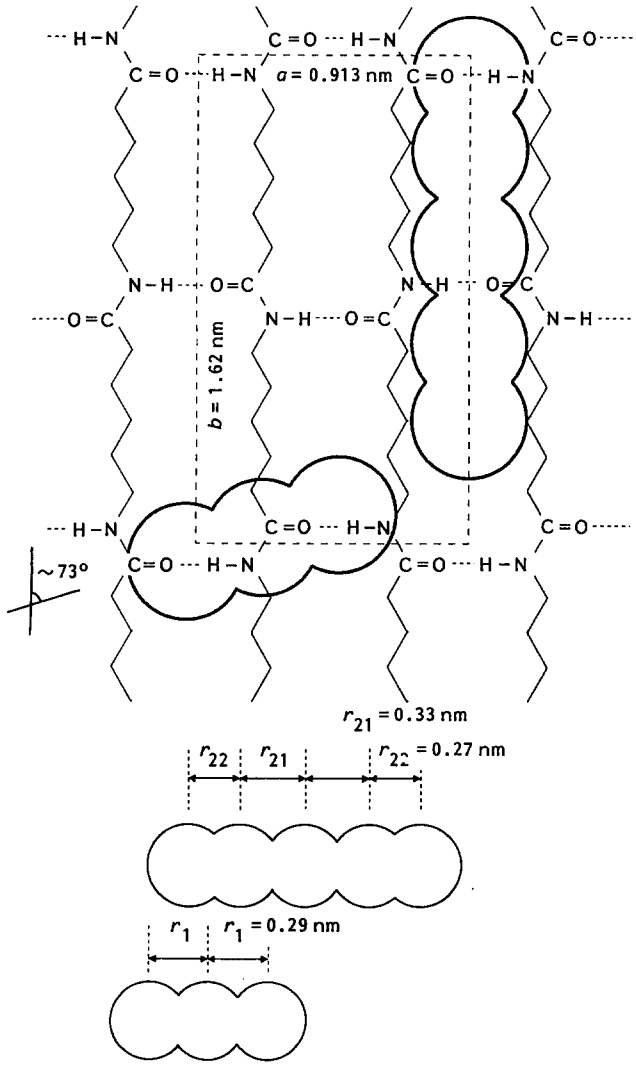

Figure 6 Schematic illustration of I_3^- (incl) and linear I_5^- ions co-ordinated to hydrogen bonds in nylon 6: $r_1 = 0.29$ nm in I_3^- and $r_{21} = 0.33$ nm, $r_{22} = 0.27$ nm in I_5^- (rectangle indicates unit cell of complex crystal)

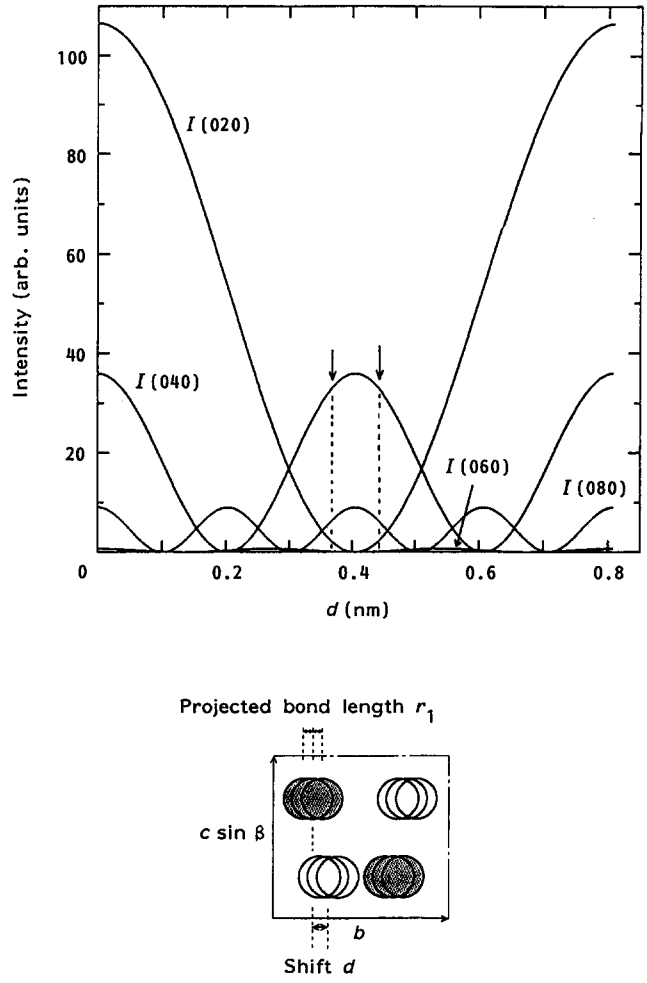

Figure 7 Calculated intensity $I(k)$ ($k = 2, 4, 6, 8$) *versus* shift d, distance between two independent I_3^- (incl) ions in a unit cell with space group of $P2_1$; arrows indicate best-fit values, $d = \sim 0.37$ and 0.44 nm (I–I bond length projected to chain axis: $r_1 = 0.085$ nm)

planes in the α-form of nylon 6 are staggered along the *b*-axis with the shift of (3/14)*b* (~0.36 nm)[1]. This value may correspond to one of the best-fitted parameters in *Figure 7*.

Neither in the complex crystal nor in the unstable one-dimensional structure can the linear I_5^- ions be accommodated. It is therefore proposed that I_5^- ions should be in the stable one-dimensional structure. The stable structure gives a strong streak on the layer line at 3.3 nm^{-1}; the value of 3.3 nm^{-1} is almost exactly the reciprocal of the average separation distance of iodine atoms in a linear I_5^- ion (0.3 nm).

The length of the long axis of a linear I_5^- ion is ~1.6 nm which is approximately that of the *b*-axis of the complex crystal. This correspondence may stabilize the linear I_5^- ion which is a minor component of iodide in an I_2–KI aqueous solution. On the other hand, the distances between the hydrogen bonds along the chain axis in the α-form have two values, 0.80 nm and 0.92 nm (*Figure 6*). Hence the length of an I_5^- ion (1.6 nm) is too long for an I_5^- ion to have a specific position along the chain axis; at any position, an I_5^- ion can be stabilized in the complex by co-ordination with two hydrogen bonds. The linear array of I_5^- ions therefore does not have a correlation

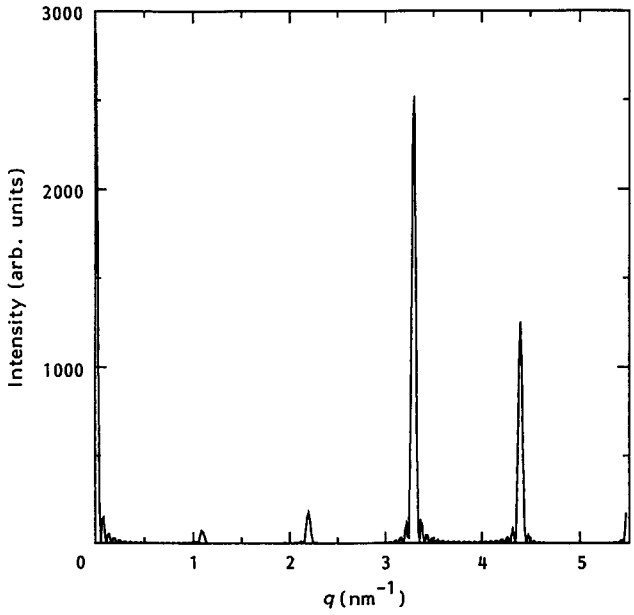

Figure 8 Calculated intensity with array of I_3^- (incl) ions ordered in a period of 0.91 nm (projected I–I distance, 0.27 nm, and $N = 20$) *versus* q ($= 2 \sin \theta / \lambda$)

with neighbouring linear arrays through hydrogen bonding; a one-dimensional structure ordered along the chain axis is thus attained.

The change in the intensities of equatorial Bragg reflections with ageing indicates change in density of iodine atoms intercalated between the hydrogen-bonded planes of nylon 6. The increase in space between the hydrogen-bonded planes with doping is assumed to be the same for the unstable structure, the stable structure and the complex crystal. Decrease in the intensities of the $00l$ reflections for odd l with ageing corresponds to the transition from the unstable structure to the complex crystal. Therefore I_3^-(incl) ions are intercalated equivalently between all hydrogen-bonded planes in the complex crystal, while the density of polyiodides intercalated in the unstable structure is fluctuated with a period that is twice the spacing between hydrogen-bonded planes. The definite three-dimensional structure is yet to be studied.

The I_3^- ion is expected to be inclined not only in the complex crystal but also in co-ordination as an independent ion without the order. The row-line streaks perpendicular to the a-axis lie at 3.2 and 4.4 nm^{-1} off the meridian: the 3rd and 4th orders of the reciprocal of the length of the a-axis (0.91 nm). Hence these row-line streaks can be attributed to a linear array along the a-axis. The linear array of I_3^-(incl) (projected I–I distance 0.27 nm in a period of 0.91 nm) gives strong streaks at around 3.2 and 4.4 nm^{-1} as shown in *Figure 8*, where N is a number of scatterers, I_3^-.

It is interesting to investigate the transition from the unstable structure to the complex crystal and/or the stable one-dimensional structure. A detailed study on the structure and dynamics of polyiodides will be required. Neutron scattering may be useful for this purpose.

ACKNOWLEDGEMENTS

The author expresses special thanks to Professor H. Miyaji of Kyoto University for his instructive discussion and advice and to Professor R. Kato and Dr M. Ashida of Kyoto University for the Raman spectroscopy.

REFERENCES

1 Holmes, D. R., Bunn, C. W. and Smith, D. J. *J. Polym. Sci.* 1955, **42**, 159
2 Arimoto, H., Ishibashi, M., Hirai, M. and Chatani, Y. *J. Polym. Sci. A* 1965, **3**, 317
3 Itoh, T., Miyaji, H. and Asai, K. *Jpn J. Appl. Phys.* 1975, **14**, 206
4 Parker, J. P. and Lindenmeyer, P. H. *J. Appl. Polym. Sci.* 1977, **21**, 821
5 Arimoto, H. *J. Polym. Sci. A* 1964, **3**, 2283
6 Abu-Isa, I. *J. Polym. Sci. A* 1974, **1**, 9, 199
7 Kawaguchi, A. *Polymer* 1992, **33**, 3981
8 Kawaguchi, A. *Kobunshi Kako* 1992, **41**, 553 (in Japanese)
9 Murthy, N. S., Szollosi, A. B., Sibilia, J. P. and Krimm, S. J. *J. Polym. Sci., Polym. Phys. Edn* 1985, **23**, 2369
10 Burzynski, R., Prasad, P. N. and Murthy, N. S. *J. Polym. Sci., Polym. Phys. Edn* 1986, **24**, 133
11 Murthy, N. S., Hatfield, G. R. and Glans, J. H. *Macromolecules* 1990, **23**, 1342
12 Murthy, N. S. *Macromolecules* 1987, **20**, 309
13 Cotton, F. A. and Wilkinson, G. 'Advanced Inorganic Chemistry', 4th Edn, Wiley, New York, 1989, Ch. 17
14 Marks, T. J. and Kalina, D. W. 'Extended Linear Chain Compounds', Vol. 1, Plenum Press, New York, 1982, Ch. 6
15 Kakinoki, J. and Komura, Y. *J. Phys. Soc. Jpn* 1952, **7**, 30
16 Scaringe, R. P. and Ibers, J. A. *Acta Cryst.* 1979, **A35**, 803

APPENDIX

Calculation of X-ray intensity of streaks from the structure of linear array with disorder[16]

The matrix method for disordered diffuse scattering in X-ray diffraction developed by Kakinoki and Komura[15] and extended to linear disorder by Scaringe and Ibers[16] is described.

For a random stack of n-kinds of linear cell with a length, C_k, a geometrical structure factor, F_k, and composition, ε_k ($k=1,2,3,\ldots,n$), the intensities of the layer streaks are given by the following equations as a function of q ($=2\sin\theta/\lambda$), neglecting the higher order terms of an average of a phase factor, Φ:

$$I_{\text{calc}}(q) \sim \langle FF^* \rangle + \frac{\langle F^* \rangle \langle F\Phi \rangle}{1-\langle \Phi \rangle} + \frac{\langle F \rangle \langle F^*\Phi^* \rangle}{1-\langle \Phi^* \rangle}$$

where

$$\langle FF^* \rangle = \sum_k \varepsilon_k F_k F_k^*$$

$$\langle F \rangle = \sum_k \varepsilon_k F_k$$

$$\langle \Phi \rangle = \sum_k \varepsilon_k \exp(-i\phi_k)$$

$$\langle F\Phi \rangle = \sum_k \varepsilon_k F_k \exp(-i\phi_k)$$

$$\phi_k = 2\pi q C_k$$

For the model of the unstable structure, two kinds of cell are taken into account (*Figure 5*). Accordingly, the following equations and parameters are used to give $I_{\text{calc}}(q)$:

$$F_A(q) = 3$$

$$F_B(q) = 3 + \exp(-2\pi i q r_{B1}) + \exp[-2\pi i q (r_{B1} + r_{B2})]$$

where $C_A = 0.425$ nm, $C_B = 0.95$ nm, $r_{B1} = 0.335$ nm, $r_{B2} = 0.28$ nm, $\varepsilon_A = 0.2$, $\varepsilon_B = 0.8$.